RSC Advances

PAPER

View Article Online
View Journal | View Issue

Cite this: *RSC Adv.*, 2019, **9**, 21931

Highly effective carbon-supported gold-ionic liquid catalyst for acetylene hydrochlorination

Xueyan Qi, *[ab] Weifeng Chen[c] and Jinli Zhang *[b]

Received 30th May 2019
Accepted 3rd July 2019

DOI: 10.1039/c9ra04082j

rsc.li/rsc-advances

The sulfur-containing ionic liquid (IL) trimethylsulfonium iodide (C_3H_9SI) was used to synthesize an efficient non-mercuric catalyst with $HAuCl_4 \cdot 4H_2O$ as a precursor and spherical active carbon (SAC) as a support. Various Au-IL/SAC catalysts were synthesized using the incipient wetness impregnation technique and applied to acetylene hydrochlorination. The 0.3% Au-IL/SAC catalyst showed the best catalytic performance, with an acetylene conversion of 90% at a temperature of 170 °C and gas hourly space velocity (GHSV) of 360 h^{-1} using water as the solvent. The catalyst also displayed excellent long-term stability: C_2H_2 conversion was maintained at 97% for up to 200 h (T = 170 °C, GHSV = 90 h^{-1}). Brunauer–Emmett–Teller surface area, thermogravimetric analysis, temperature programmed desorption, X-ray diffraction, transmission electron microscopy, and X-ray photoelectron spectroscopy results together showed that the C_3H_9SI additive significantly improved the dispersion of Au species and inhibited coke deposition on the catalyst surface during the acetylene hydrochlorination reaction. The superior activity and stability of the Au-IL/SAC catalyst make it a green catalyst for the industrial application of acetylene hydrochlorination.

1. Introduction

Activated carbon (AC)-supported 5–12 wt% $HgCl_2$ is a frequently used industrial catalyst for the acetylene hydrochlorination reaction used to manufacture vinyl chloride monomer (VCM), which is the important chemical intermediate in the synthesis of polyvinyl chloride (PVC). However, due to continuing efforts to protect the environment, the use of $HgCl_2$ has been increasingly limited, and its use for the synthesis of VCM has been prohibited since 2013; moreover, a comprehensive mercury-free ban is scheduled to be implemented in 2022.[1] It is thus urgent to search for an alternative mercury-free catalyst for the acetylene hydrochlorination reaction.

Many efforts have been made in researching and developing such mercury-free catalysts. According to the relationship between the standard electrode potentials of various metal chloride catalysts and their activities, Hutchings and co-workers found that gold can effectively catalyze the acetylene hydrochlorination reaction.[2,3] First the single-component gold-based catalyst was studied,[4–8] and then the catalyst was modified with multiple components in order to enhance its activity[9–14]

However, Au-based catalysts have still not been used on a large scale due to their high cost and instability. Many researchers have been investigating non-precious metals, and even nonmetallic materials as catalysts of the reaction.[15–20] While they are less expensive than the Au-based catalysts, their catalytic activities are also much lower. Therefore, the study of catalysts with gold as the active component was also the main focus for acetylene hydrochlorination. In recent years, gold complex catalysts such as the Au-GSH complex and $AuPPh_3Cl$ complex have been designed.[21–23] Note that sulfur-containing ligands have been shown by Hutchings and co-workers to stabilize Au(I) catalysts.[23] The stable cationic gold was shown to be present in the form of gold–sulfur bonds and to be highly dispersed in the catalyst. They also illustrated that even sulfur-containing ligands dissociated, and the presence of the sulfur moiety may serve to immobilize/anchor the Au and help prevent reduction and sintering of Au. The gold complex catalyst exhibited superefficient catalytic activity and stability even when the amount of gold loaded was reduced to 0.1 wt% at 500 h^{-1}.

Recently, the use of ionic liquids (ILs) as green solvents and catalysts has been receiving increasing attention.[24–26] It has been shown that IL films could—due to their excellent solubility, low volatility and high thermal stability—be used to dissolve transition-metal complexes. As a thin film on the catalyst surface, an IL provides a homogeneous solvent environment that stabilizes the metal cation and accelerates mass transfer for the transition metal catalyst.[27] Zhao *et al.* reported that the Au(III)-IL/AC catalyst with 1-propyl-3-methylimidazolium chloride as the ionic liquid for acetylene hydrochlorination exhibited a relatively high catalytic performance of about 77.1% for

[a]*College of Materials Science and Engineering, Hebei University of Engineering, Handan 056038, Hebei, PR China. E-mail: qixueyan001@163.com*

[b]*School of Chemical Engineering and Technology, Tianjin University, Tianjin 300072, PR China. E-mail: zhangjinli@tju.edu.cn*

[c]*The 718th Research Institute of China Shipbuilding Heavy Industry Corporation, Handan 056027, Hebei, PR China. E-mail: chen228@tju.edu.cn*

C_2H_2 conversion.[28] Li *et al.* investigated Ru-IL/AC catalysts using the supported ionic liquid phase (SILP) technique for acetylene hydrochlorination, and the best catalyst was 1% Ru@15% TPPB/AC, which showed excellent acetylene conversion of 99.7% under the reaction conditions of 170 °C, GHSV (C_2H_2) of 360 h^{-1}, and $V_{(HCl)}/V_{(C_2H_2)} = 1.5$.[27] All of these results showed that the IL could significantly stabilize the metal oxidation state and prevent the formation of agglomerate. On the other hand, it is worth mentioning that the oxidizing *aqua regia* or hydrochloric acid is often used as a solvent to ensure that the catalyst contains a relatively high number of cationic Au species during the preparation process and the reaction. However, aqua regia or hydrochloric acid are corrosive and may hence be harmful to exposed workers and equipment. Some of these catalysts when used with water as the solvent show decreased catalytic activity because the catalysts contain in this case a relatively high amount of Au^0. Considering the excellent catalytic performance and preparation methods of IL catalysts, it is necessary to continue to investigate producing more efficient ILs, convenient preparation methods, and environmentally friendly gold-based catalysts for acetylene hydrochlorination.

In the current work, sulfur-bearing ILs were adopted with water as the solvent to prepare Au-IL/spherical activated carbon (SAC) catalysts using the incipient wetness impregnation method, and these catalysts were assessed for acetylene hydrochlorination. The trimethylsulfonium iodide additive provided the sulfur atom that increased the electron density of the Au^{3+} center *via* the transfer of the lone pair of electrons from the sulfur atom to the Au^{3+} center. On the other hand, there was an electrostatic interaction of cationic gold with the iodine anion. Au^{3+} species have been shown to serve as electron donors in the HCl adsorption process,[29] and it was, therefore, most likely that this feature promoted the ability of Au-IL/SAC catalysts to adsorb a relatively high amount of hydrogen chloride and stabilize cationic gold during the reaction. The Au-IL/AC catalyst exhibited high catalytic activity, specifically with 90% acetylene conversion, 38% more than that of the catalyst without IL. The results indicated that the IL additive could substantially improve the dispersion of gold species, enhance the adsorption of HCl and inhibit the coke deposition.

2. Experimental

2.1 Materials

$HAuCl_4 \cdot 4H_2O$ (Au content ≥ 47.8%) was purchased from Alfa Aesar; trimethylsulfonium iodide (C_3H_9SI, purity ≥ 98%) was supplied by Tianjin Xiensi Bio-Chem Technology Development Co., Ltd., and spherical activated carbon (SAC, neutral, pitch-based, 20–40 mesh) was purchased from ShangHai Carbosino Material Co., Ltd. All of the other materials and chemicals were commercially available and were used without further purification.

2.2 Catalyst preparation

Au-IL/SAC catalysts were prepared *via* the incipient wetness impregnation method. An $HAuCl_4$ aqueous solution (10 ml, 0.00121 mol L^{-1} or 0.00363 mol L^{-1}) was added dropwise to 5 g of SAC under stirring, and then steeped for 12 h at room temperature, followed by the desiccation of this mixture in a water bath at 60 °C for 10 h. Then, an aqueous solution of C_3H_9SI (10 ml) was added to the above mixture under constant stirring. The mixture was set aside for 10 h, evaporated in a steam bath, and then dried at 120 °C for 12 h. The resultant catalyst was named Au-10% IL/SAC. For comparison, the Au/SAC catalyst was also prepared under the same conditions as described above. Additionally, the dip order of gold and C_3H_9SI was changed to obtain the 10% IL-Au/SAC catalyst. Other gold-based catalysts with various relative amounts of C_3H_9SI from 5 wt% to 30 wt% were prepared. Au loading in all of the Au-based catalysts was fixed at 0.1 wt% or 0.3 wt%.

2.3 Catalytic performance tests

The catalytic performance test was carried out in a fixed-bed micro-reactor (i.d. of 10 mm). A CKW-1100 temperature controller (Chaoyang Automation Instrument Factory, Beijing, China) was used to control the temperature of the reaction. Acetylene (gas, 99.9% purity) was treated using a silica-gel desiccant to remove trace impurities, and hydrogen chloride (gas, 99.9% purity) was passed through 5A molecular sieves for drying. Nitrogen was purged into the reactor to remove the air and water in the system before the reaction. The catalyst was activated by hydrogen chloride gas with a flow rate of 25 mL min^{-1} for 30 min. Hydrogen chloride and acetylene with a molar ratio of 1.2 (C_2H_2: 16.6 mL min^{-1}, HCl: 20.3 mL min^{-1}) were introduced into the reactor containing 3 mL of the catalyst until the reaction temperature reached 170 °C. A 360 h^{-1} C_2H_2 gas hourly space velocity (GHSV) was achieved by controlling the calibrated mass flow meters. The reactor effluent stream was passed through an absorption bottle containing an aqueous solution of NaOH to remove superfluous HCl and then the gas mixture was analyzed online by using a BeiFen 3420A gas chromatograph.

2.4 Catalyst characterizations

The BET pore structure and specific surface areas were investigated by using a Quantachrome Autosorb Automated Gas Sorption System (Quantachrome Instruments, USA). The samples were degassed at 160 °C for 4 h, and then analyzed *via* liquid nitrogen adsorption at −196 °C.

Thermogravimetric analysis (TGA) was carried out using a TG-DTA 2 thermal analyzer (METTLER TOLEDO, Switzerland) under an air atmosphere with a flow rate of 60 mL min^{-1}. The temperature was increased from 35 °C to 900 °C with a heating rate of 10 °C min^{-1}.

X-ray diffraction (XRD) patterns were collected on a D8-Focus diffractometer using Cu Kα radiation ($\lambda = 1.5406$ Å) at a scanning rate of 5 °C min^{-1}, with 2θ ranging from 10° to 90°.

Temperature-programmed desorption (TPD) experiments were performed using an AutoChem BET TPR/TPD (Quantachrome Instruments AMI-90). First, the catalysts (150 mg) were treated with C_2H_2 and HCl gas for 4 h at the reaction temperature in the reactor. The catalysts, after having adsorbed these

species, were treated with He gas at 30 °C for 30 min, and then the temperature was increased from 30 °C to 900 °C under an He gas atmosphere. For the C_2H_3Cl-TPD, the C_2H_3Cl gas was adsorbed by the samples on a TPD instrument for 1 h at 170 °C and then the desorption procedure was carried out as described above.

Transmission electron microscopy (TEM) was carried out using a JEM 2100F electron microscope. The catalyst in powder form was first dispersed in ethanol and the resulting suspension was added dropwise onto carbon-film-coated copper TEM grids, which were then used to obtain the images.

X-ray photoelectron spectroscopy (XPS) data were obtained using a Thermo ESCALAB 250Xl (Thermo Fisher Scientific, USA), with a monochromatic Al Kα X-ray source (225 W). The binding energies were adjusted by referencing the C (1s) level at 284.4 eV.

3. Results and discussion

3.1 Performance of Au-based catalysts

Fig. 1(a) shows the catalytic performance of the Au-10% IL/SAC catalyst, and the corresponding performances of SAC, IL/SAC, Au/SAC and 10% IL-Au/SAC materials for comparison. The acetylene conversion of SAC was initially 25% and then decreased to 22% in 24 h. 10% IL/SAC exhibited higher activity than did SAC at the beginning of reaction, but nearly the same activity as did SAC after 24 h. These results showed that the individual IL/SAC sample contributed very little to the activity. For the pristine Au/SAC (0.1 wt% Au) catalyst, the acetylene conversion decreased from 80% to 47% after 24 h of reaction at 170 °C. The Au-10% IL/SAC showed the highest catalytic activity of 84% and only a reduction of 6% after 24 hours of reaction. It should be noted that the Au-based catalysts displayed a significant increase of C_2H_2 conversion after adding the IL. The 10% IL-Au/SAC catalyst showed the lowest initial activity of all the Au-based catalysts, with a conversion of 74% at 3 h and 48% at 24 h. While the conversion of the 10% IL-Au/SAC was higher than that of Au/SAC within the first 20 hours, it showed poor stability. For loadings of C_3H_9SI between 5% and 30%, *i.e.*, when using Au-5% IL/SAC, Au-10% IL/SAC, Au-20% IL/SAC and Au-30% IL/SAC catalysts, acetylene conversions of 79%, 79%, 84% and 74% were achieved, and decreased to 76%, 77%, 82% and 70%, respectively, after the 24 hours of the reaction (Fig. 1(b)). These results indicated that the C_3H_9SI additive can be used to improve the activity of Au-based catalysts, and in our experiments the Au-20% IL/SAC catalyst showed the best activity of all of the catalysts.

After adopting the optimal dipping order and the optimal C_3H_9SI loading level, the Au loading was increased from 0.1 wt% to 0.3 wt% in order to obtain more convincing characterization results. The C_2H_2 conversions of these catalysts are shown in Fig. 2. The 0.3% Au/SAC catalyst showed an acetylene conversion of 65% after 3 h. The optimum acetylene conversion over 0.3% Au-IL/SAC catalyst was 90% with a steady 100% selectivity for VCM. The C_2H_2 conversion of the 0.3% Au-IL/SAC catalyst was 35% higher than that of the sample without ionic liquid after 24 hours. These results suggested that the IL additive can markedly improve the activity and selectivity of gold catalysts for acetylene hydrochlorination.

3.2 Catalyst characterizations

3.2.1 BET results. The pore structure parameters of the catalysts were investigated by carrying out low-temperature N_2 adsorption/desorption experiments. As listed in Table 1, the SAC support showed type-I isotherms and the bare SAC displayed a specific surface area of 1149 $m^2\ g^{-1}$ and a total pore volume of 0.661 $cm^3\ g^{-1}$. After the loading of gold species and IL, the surface area and total pore volume of the SAC decreased, indicating that the carrier channel was blocked by the active gold species or the C_3H_9SI.[30] Comparing the data indicated that the used catalysts exhibited lower surface areas and total pore volume than did the fresh catalyst after 24 h of the reaction. For the used 0.3% Au/SAC catalyst, the surface area decreased by about 10%, from an initial value of 956 $m^2\ g^{-1}$ to 860 $m^2\ g^{-1}$. Likewise, the surface area of the used 0.3% Au-IL/SAC catalysts decreased by about 7%. The particular variations are shown in Table 1. For the 0.3% Au/SAC catalyst, the amplitude of

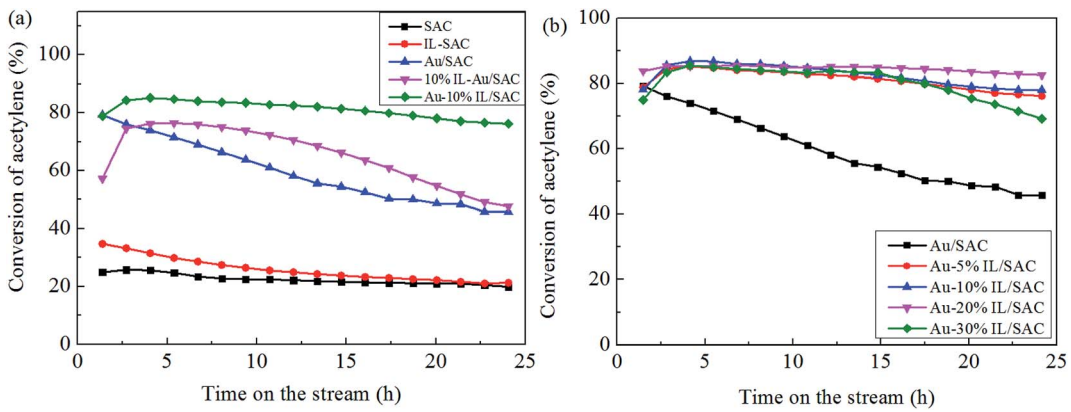

Fig. 1 The acetylene conversions of Au-IL catalysts with different dipping orders (a) and different ionic liquid loading levels (b). Reaction conditions: $T = 170$ °C, C_2H_2 gas hourly space velocity (GHSV) = 180 h^{-1}, feed volume ratio $V_{(HCl)}/V_{(C_2H_2)} = 1.2$, 0.1 wt% Au.

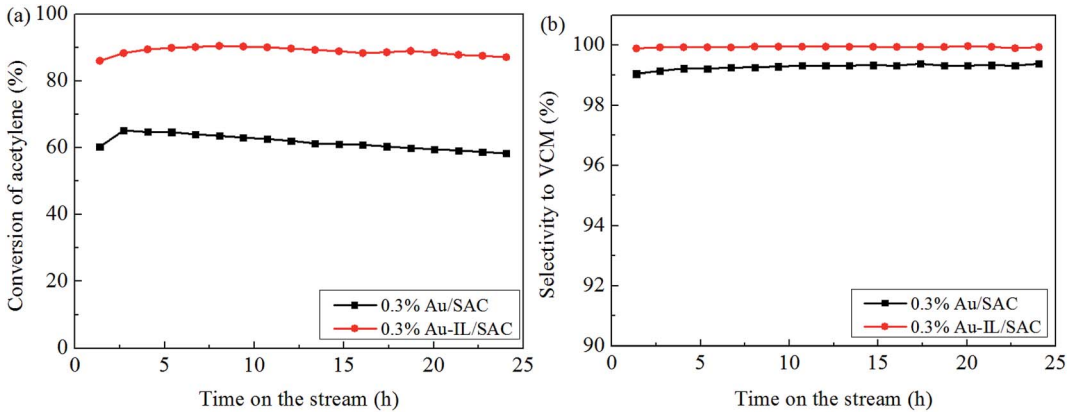

Fig. 2 The acetylene conversion and selectivity for VCM of 0.3% Au/SAC and 0.3% Au-IL/SAC catalysts. Reaction conditions: $T = 170$ °C, C_2H_2 gas hourly space velocity (GHSV) = 360 h^{-1}, feed volume ratio $V_{(HCl)}/V_{(C_2H_2)} = 1.2$, 0.3 wt% Au.

Table 1 Pore structure parameters of the fresh and used Au-based catalysts

	S_{BET} (m^2 g^{-1})		Total pore volume (cm^3 g^{-1})			
Catalyst	Fresh	Used	Fresh	Used	ΔS_{BET}%	ΔV%
SAC	1149	1055	0.661	0.612	8.2	7.4
0.3% Au/SAC	956	860	0.464	0.413	10	11
0.3% Au-IL/SAC	825	768	0.402	0.377	7	6.2

variation of S_{BET} (ΔS_{BET}) and that of V (ΔV) were measured to be 10% and 11%. The 0.3% Au-IL/SAC catalyst showed lower surface area and pore volume variations than did 0.3% Au/SAC, specifically values of 7% and 6.2% for ΔS_{BET} and ΔV, respectively. These results, combined with the trend of the variations of the activity and BET data for the catalysts, indicated that the variation was probably due to catalyst sintering or carbon deposition during the reaction.[31]

3.2.2 Coking deposition analysis. TGA was performed to measure the amount of coke deposited over the 0.3% Au/SAC and 0.3% Au-IL/SAC catalysts. As seen in Fig. 3 and Table 2, all of the catalysts showed a slight weight loss as the temperature was increased up to 150 °C, attributed to water desorption from the surfaces of catalysts. The fresh 0.3% Au/SAC catalyst displayed a weight loss of about 3.4% as the temperature was increased from 150–556 °C. In this same temperature range, the used 0.3% Au/SAC catalyst underwent a more marked weight loss (7.5%), attributed to the burning of deposited carbon and carbon-containing groups during the acetylene hydrochlorination reaction. The TGA curves of the fresh and used 0.3% Au-IL/SAC catalysts showed mass losses of, respectively, 4.6% and 6.7% as the temperature was increased from 150 °C to 556 °C. Both the fresh and used catalysts showed rapid weight losses after 556 °C, attributed to the combustion of activated carbon.

Coke deposition was calculated using the previously described method,[12] and the computed results are listed in Table 2. The relative amount of deposited coke was 4.3% for the 0.3% Au/SAC catalyst and 2.1% for the 0.3% Au-IL/SAC catalyst after 24 h of reaction. The trend here was similar to that for the BET results, as coke deposition in general causes losses of both surface area and pore volume. Therefore, we concluded that the C_3H_9SI additive inhibited the formation of coke deposits, and that this inhibition enhanced the catalytic activity.

3.2.3 Adsorption properties of the fresh catalysts. TPD profiles were plotted to explore the adsorption properties of the

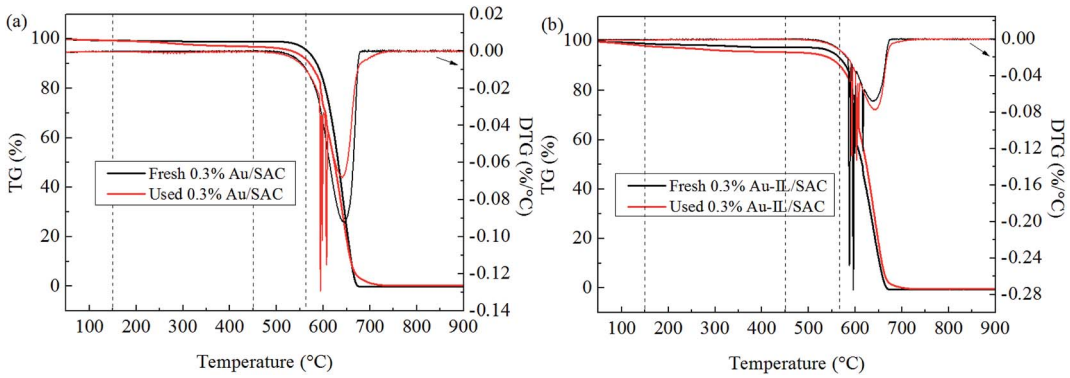

Fig. 3 TG and DTG curves of the fresh and used 0.3% Au/SAC and 0.3% Au-IL/SAC catalysts.

Table 2 Carbon deposition on the 0.3% Au/SAC and 0.3% Au-IL/SAC catalysts

Catalysts	Amount of carbon deposition (%)
0.3% Au/SAC	4.1
0.3% Au-IL/SAC	2.1

reactants and the product of the fresh catalysts. Generally, the peak area represents adsorption ability and desorption temperature reflects adsorption strength. Fig. 4(a) displays the C_2H_2-TPD profiles of the fresh 0.3% Au/SAC and 0.3% Au-IL/SAC catalysts. Both of the catalysts yielded an obvious desorption peak of acetylene in the temperature range 100–450 °C. For the 0.3% Au/SAC catalyst, the desorption temperature was 210 °C, a value 10 °C lower than that for the 0.3% Au-IL/SAC sample. The desorption area of acetylene for the 0.3% Au-IL/SAC catalyst was greater than that for the fresh 0.3% Au/SAC sample. These results taken together indicated that the C_3H_9SI additive enhanced the ability of the sample to adsorb C_2H_2. The HCl-TPD profiles are shown in Fig. 4(b). All of the catalysts yielded two HCl desorption peaks, which may have been due to physical adsorption at the low-temperature range and chemical adsorption at the high-temperature range. The HCl desorption area of the 0.3% Au-IL/SAC catalyst was considerably larger than that of 0.3% Au/SAC sample, indicating that the 0.3% Au-IL/SAC catalyst strongly adsorbed HCl. As for the product VCM, the result was found to be opposite that of the HCl reactant. As shown in Fig. 4(c), the two catalysts showed markedly different VCM desorption areas. The VCM area of the 0.3% Au-IL/SAC catalyst was measured to be less than that of the 0.3% Au/SAC catalyst. These results suggested a relatively rapid diffusion of the products out of the catalyst channel, hence lessening the occurrence of carbon deposition. In summary, the addition of C_3H_9SI to the catalyst not only enhanced the adsorption of the reactants, especially HCl, but also promoted desorption of the VCM product. The TPD results combined with the DTA results provided powerful evidence that adding C_3H_9SI to the Au-based catalyst can inhibit the deposition of coke during the reaction.

3.2.4 Valence change of the active component. Fig. 5 shows the XRD patterns of the fresh and used Au-based catalysts. Apart from the amorphous diffraction peaks and the typical coal peaks of the SAC, a diffraction peak at 38.08° was detected for the fresh 0.3% Au/SAC catalyst and was assigned to the (111) planes of metallic Au^0. This result indicated that the preparation process led to the reduction of Au^{3+} to Au^0. For the used 0.3% Au/SAC catalyst, the intensity of the Au reflection at 38.08° was observed to be even more intense, indicating additional reduction from Au^{3+} to Au^0 during the reaction. Besides the amorphous diffraction peaks of carbon, no discernible reflection was detected for the fresh 0.3% Au-IL/SAC catalysts, not even in the used sample, indicating the high dispersion of active species. These results clearly indicated that the addition of IL suppressed the reduction of Au^{3+} to Au^0 and improved the dispersion of active species, not only in the preparation process but also during the reaction.

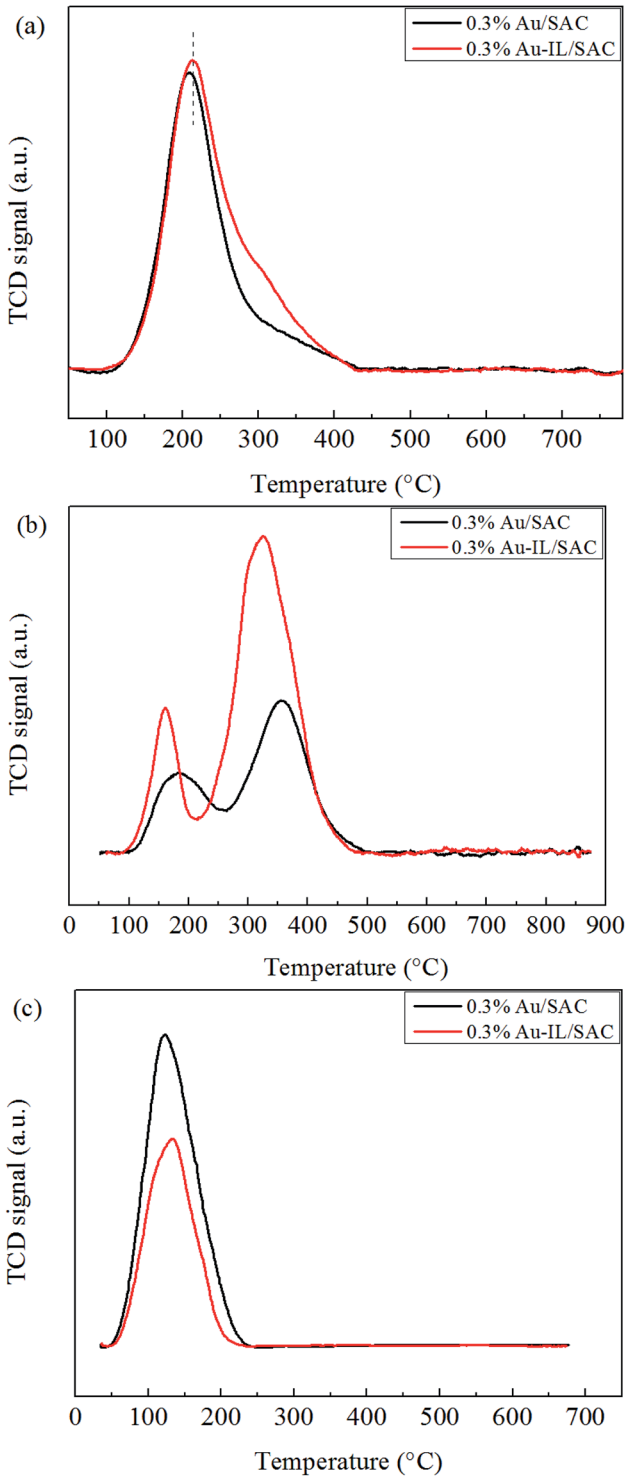

Fig. 4 TPD profiles of the fresh 0.3% Au/SAC and 0.3% Au-IL/SAC catalysts for (a) C_2H_2-TPD, (b) HCl-TPD, and (c) VCM-TPD.

TEM images were obtained to gain more information about the particle size and dispersion of Au species, as shown in Fig. 6. The average particle dimensions were measured from these images to be 3.0 nm and 3.3 nm for the fresh and used 0.3% Au/SAC catalysts. The pitch-based activated carbon has better catalytic activity than do

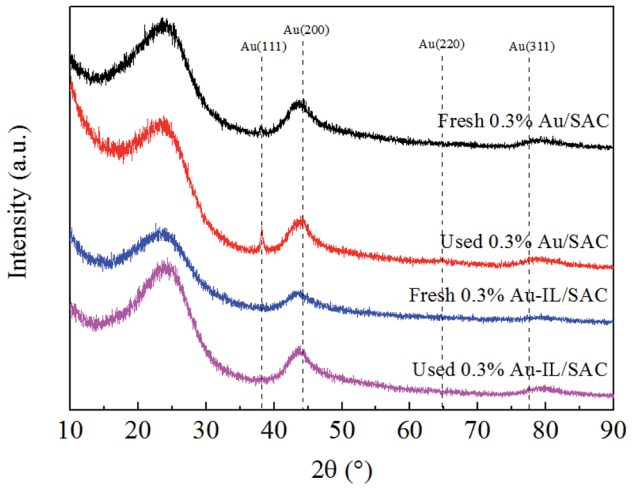

Fig. 5 XRD patterns of 0.3% Au/SAC and 0.3% Au-IL/SAC catalysts.

coconut shell-based activated carbon and coal-based activated carbon. Therefore, after short reaction times, the gold particle dimensions were less than 4 nm whether fresh or used 0.3% Au/SAC catalyst was deployed. For the fresh and used 0.3% Au-IL/SAC catalysts, the particle dimensions were 1.2 nm and 1.3 nm, respectively. It was reasonable to conclude that the addition of IL made the gold species highly dispersed on the surface of the support, effectively preventing the reduction of Au^{3+} to Au^0.

XPS spectra were acquired to monitor the valence state and relative amount of gold species for the fresh and used Au-based catalysts. Typical XPS spectra in the region of the Au 4f orbital for 0.3% Au/SAC and 0.3% Au-IL/SAC are shown in Fig. 7. These data indicated that both Au^{3+} and Au^0 co-existed in the fresh and used catalysts.

Table 3 lists the binding energies and the relative amounts of Au species. For the fresh 0.3% Au/SAC, peaks at binding energy values of 86.5 eV and 84.3 eV were observed, and were attributed to Au^{3+} and Au^0, respectively. According to the XPS data of the fresh catalysts, the presence of the C_3H_9SI additive reduced the binding energy of Au^{3+} by 0.1 eV, while that of Au^0 increased by 0.1 eV. This result indicated that electron transfer indeed occurred and that

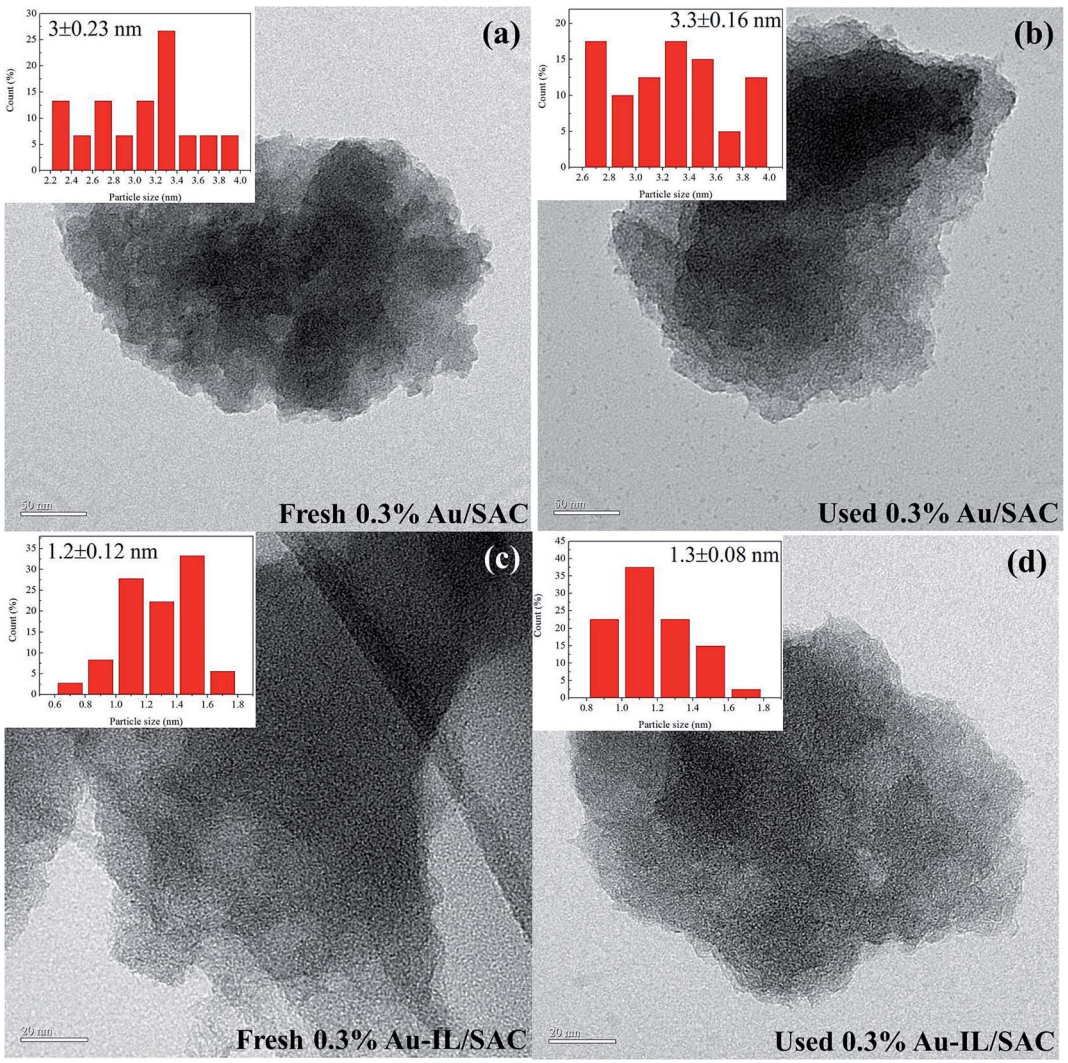

Fig. 6 TEM images of the fresh and used 0.3% Au/SAC and 0.3% Au-IL/SAC catalysts.

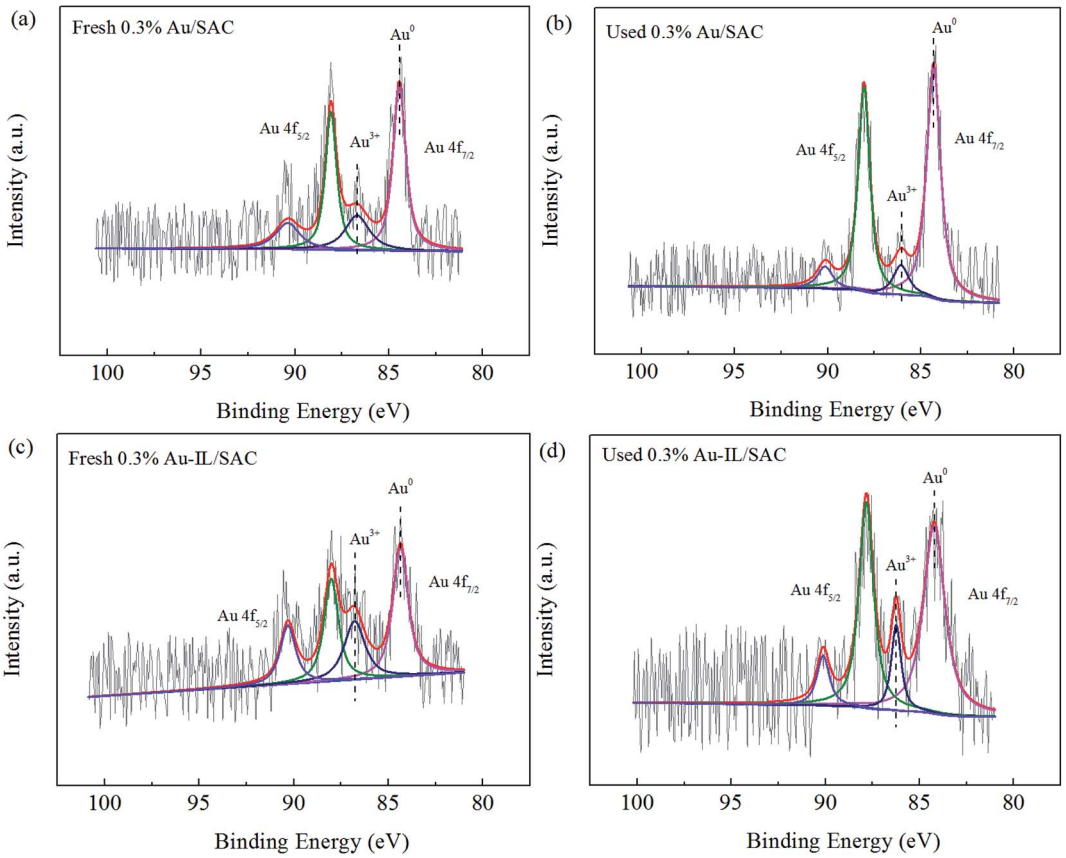

Fig. 7 High-resolution XPS spectra in the Au 4f region for the fresh and used 0.3% Au/SAC and 0.3% Au-IL/SAC catalysts.

Table 3 Relative amounts and binding energies of gold species in 0.3% Au/SAC and 0.3% Au-IL/SAC catalysts

	Au species (%)		Binding energies (eV)	
Catalyst	Au^{3+}	Au^0	Au^{3+}	Au^0
Fresh 0.3% Au/SAC	28.7	71.3	86.5	84.3
Used 0.3% Au/SAC	12.5	87.5	86.3	84.3
Fresh 0.3% Au-IL/SAC	38	62	86.4	84.4
Used 0.3% Au-IL/SAC	25.5	74.5	86.3	84.3

there was a strong interaction between the gold species and C_3H_9SI additive. For the fresh 0.3% Au/SAC and 0.3% Au-IL/SAC catalysts, the relative amounts of the active component Au^{3+} were 28.7% and 38.0%, respectively. The used 0.3% Au/SAC catalyst had a relatively large amount (87.5%) of metallic Au^0 and hence low amount (12.5%) of Au^{3+} species. However, the 0.3% Au-IL/SAC catalyst showed fewer Au^{3+} ions reduced to Au^0 than did 0.3% Au/SAC after the reaction. This result showed that the IL additive suppressed the reduction of Au^{3+} to Au^0 during the reaction and improved the catalytic activity, in accordance with the results of the XRD and TEM analyses.

3.2.5 Long-term stability testing. The Au-IL/SAC catalyst was subjected to a long-term stability testing, specifically for more than 200 h, under the reaction conditions of 170 °C, the GHSV (C_2H_2) of 90 h^{-1} and $V_{HCl}/V_{C_2H_2} = 1.2$. As shown in Fig. 8, the acetylene conversion decreased just from 97% to 95% after more than 200 h of reaction. This result provided evidence for the suitability of the Au-IL/SAC catalyst for long-term tests and industrial production needs.

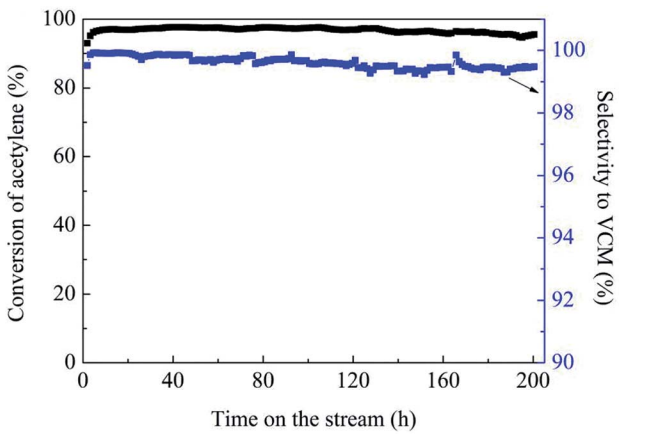

Fig. 8 Long-term stability testing of the 0.3% Au-IL/SAC catalyst. Reaction conditions: temperature (T) = 170 °C, C_2H_2 gas hourly space velocity (GHSV) = 90 h^{-1}, feed volume ratio $V_{(HCl)}/V_{(C_2H_2)} = 1.2$, 0.3 wt% Au.

4. Conclusions

In summary, Au-IL/SAC catalysts were prepared and assessed for the acetylene hydrochlorination reaction. Compared to the 0.3% Au/SAC catalyst, the 0.3% Au-IL/SAC catalyst exhibited obviously better catalytic performance. Under the conditions of temperature = 170 °C, $V_{(HCl)}/V_{(C_2H_2)} = 1.2$, and GHSV $(C_2H_2) = 360\ h^{-1}$, the 0.3% Au-IL/SAC catalyst showed the best performance, with an acetylene conversion of 90% and the selectivity for VCM of 100%. The characterizations indicated the ability of the IL additive to effectively inhibit carbon deposition of the catalyst, simultaneously improve the dispersion of gold species, and enhance the amounts of acetylene and especially hydrogen chloride adsorbed on the catalyst. In addition, the interaction between gold and IL was indicated to stabilize the high valence state of the Au species and endow the catalyst with long-term stability. The optimized catalyst thus has the potential for use in industrial production due to its advantageous low cost, ease of preparation, and non-polluting character.

Conflicts of interest

There are no conflicts to declare.

Acknowledgements

We gratefully acknowledge the financial support of the Major State Basic Research Development Program (No. 2012CB720302) and NSFC (21176174).

References

1 G. Malta, S. J. Freakley, S. A. Kondrat and G. J. Hutchings, *Chem. Commun.*, 2017, **53**, 11733–11746.
2 G. J. Hutchings, *J. Catal.*, 1985, **96**, 292.
3 G. J. Hutchings and D. T. Grady, *Appl. Catal.*, 1985, **17**, 155.
4 B. Nkosi, M. D. Adams, N. J. Coville and G. J. Hutchings, *J. Catal.*, 1991, **128**, 378–386.
5 M. Conte, A. F. Carley, G. Attard, A. A. Herzing, C. J. Kiely and G. J. Hutchings, *J. Catal.*, 2008, **257**, 190–198.
6 M. Conte, A. F. Carley, C. Heirene, D. J. Willock, P. Johnston, A. A. Herzing, C. J. Kiely and G. J. Hutchings, *J. Catal.*, 2007, **250**, 231–239.
7 M. Conte, A. F. Carley and G. J. Hutchings, *Catal. Lett.*, 2008, **124**, 165–167.
8 M. Conte, C. J. Davies, D. J. Morgan, T. E. Davies, A. F. Carley, P. Johnston and G. J. Hutchings, *Catal. Sci. Technol.*, 2013, **3**, 128.
9 S. Wang, B. Shen and Q. Song, *Catal. Lett.*, 2010, **134**, 102.
10 H. Zhang, W. Li, X. Li, W. Zhao, J. Gu, X. Qi, Y. Dong, B. Dai and J. Zhang, *Catal. Sci. Technol.*, 2015, **5**, 1870.
11 K. Zhou, W. Wang, Z. Zhao, G. Luo, J. T. Miller, M. Wong and F. Wei, *ACS Catal.*, 2014, **4**, 3112.
12 G. Li, W. Li and J. Zhang, *Catal. Sci. Technol.*, 2016, **6**, 3230.
13 Y. Pu, J. Zhang, X. Wang, H. Zhang, L. Yu, Y. Dong and W. Li, *Catal. Sci. Technol.*, 2014, **4**, 4426.
14 Y. Dong, H. Zhang, W. Li, M. Sun, C. Guo and J. Zhang, *J. Ind. Eng. Chem.*, 2016, **35**, 177.
15 X. Li, Y. Wang, L. Kang, M. Zhu and B. Dai, *J. Catal.*, 2014, **311**, 288–294.
16 X. Li, X. Pan, L. Yu, P. Ren, X. Wu, L. Sun, F. Jiao and X. Bao, *Nat. Commun.*, 2014, **5**, 3688–3694.
17 K. Zhou, J. Si, J. Jia, J. Huang, J. Zhou, G. Luo and F. Wei, *ChemSusChem*, 2014, **4**, 7766–7769.
18 K. Zhou, B. Li, Q. Zhang, J. Huang, G. Tian, J. Jia, M. Zhan, G. Luo, D. Su and F. Wei, *ChemSusChem*, 2014, **7**, 723–728.
19 J. Zhao, Y. Yu, X. Xu, S. Di, B. Wang, H. Xu, J. Ni, L. Guo, Z. Pan and X. Li, *Appl. Catal., B*, 2017, **206**, 175–183.
20 B. Dai, K. Chen, Y. Wang, L. Kang and M. Zhu, *ACS Catal.*, 2015, **5**, 2541–2547.
21 X. Qi, W. Li, J. Gu, C. Guo and J. Zhang, *RSC Adv.*, 2016, **6**, 105110–105118.
22 Y. Dong, W. Li, Z. Yan and J. Zhang, *Catal. Sci. Technol.*, 2016, **6**, 7946–7955.
23 P. Johnston, N. Carthey and G. J. Hutchings, *J. Am. Chem. Soc.*, 2015, **137**, 14548–14557.
24 J. F. Wishart, *Energy Environ. Sci.*, 2009, **2**, 956.
25 L. Han, S. W. Park and D. W. Park, *Energy Environ. Sci.*, 2009, **2**, 1286.
26 J. Hu, Q. Yang, L. Yang, Z. Zhang, B. Su, Z. Bao, Q. Ren, H. Xing and S. Dai, *ACS Catal.*, 2015, **5**, 6724–6731.
27 S. Shang, W. Zhao, Y. Wang, X. Li, J. Zhang, Y. Han and W. Li, *ACS Catal.*, 2017, **7**, 3510–3520.
28 J. Zhao, S. Gu, X. Xu, T. Zhang, Y. Yu, X. Di, J. Ni, Z. Pan and X. Li, *Catal. Sci. Technol.*, 2016, **6**, 3263–3270.
29 J. Zhao, T. Zhang, X. Di, J. Xu, J. Xu, F. Feng, J. Ni and X. Li, *RSC Adv.*, 2015, **5**, 6925–6931.
30 H. Zhang, B. Dai, X. Wang, W. Li, Y. Han, J. Gu and J. Zhang, *Green Chem.*, 2013, **15**, 829.
31 B. Nkosi, N. J. Coville, G. J. Hutchings, M. D. Adams, J. Friedl and F. E. Wagner, *J. Catal.*, 1991, **128**, 366.